Fermions, quantum gravity, and holography in two dimensions

Muhammad Asaduzzaman[*]
University of Iowa, Department of Physics and Astronomy, Iowa City, 52242, Iowa, USA

Simon Catterall[†] and Abhishek Samlodia[‡]
Syracuse University, Department of Physics, Syracuse, 13244, New York, USA

(Received 1 March 2024; accepted 5 April 2024; published 10 May 2024)

We study a model comprising N flavors of Kähler Dirac fermion propagating on a triangulated two-dimensional disk which is constrained to have a negative average bulk curvature. Dirichlet boundary conditions are chosen for the fermions. Quantum fluctuations of the geometry are included by summing over all possible triangulations consistent with these constraints. We show in the limit $N \to \infty$ that the partition function is dominated by a regular triangulation of two-dimensional hyperbolic space. We use strong coupling expansions and Monte Carlo simulation to show that in this limit boundary correlators of the fermions have a power law dependence on boundary separation as one expects from holography. However, we argue that this behavior breaks down for any finite number of massive fields in the thermodynamic limit and quantum fluctuations of the bulk geometry drive the theory into a nonholographic phase. In contrast, for massless fermions, we find evidence that the boundary is conformal even for finite N. This is consistent with theoretical results in quantum Liouville theory.

DOI: 10.1103/PhysRevD.109.106010

I. INTRODUCTION

In this paper, we study the effects of fermionic matter on the partition function for two-dimensional quantum gravity. In particular we are interested in questions of holography and hence restrict our discrete geometries to triangulations with the topology of a disk. For our fermionic matter, we use Kähler-Dirac fermions rather than Dirac fermions.

Kähler-Dirac (KD) fields afford a natural way to couple lattice fermions to discrete geometry. In a continuum D-dimensional Euclidean space with metric g, a KD field Φ is composed of the set of all (Grassmann valued) antisymmetric tensor fields (p-forms)

$$\Phi = (\phi, \phi_\mu, \phi_{\mu\nu}, \ldots, \phi_{\mu_1\mu_2\ldots\mu_D}) \tag{1}$$

with the corresponding action,

$$S_{\mathrm{KD}} = \int \mathrm{d}^D x \sqrt{g} \bar{\Phi}(d - d^\dagger + m)\Phi \tag{2}$$

where d denotes the exterior derivative and the only dependence of the fermion operator on the metric arises in the definition of the adjoint operator $d^\dagger$. Notice that the square of the KD operator $(d - d^\dagger)$ is just the Hodge Laplacian. In the flat space, one can form a matrix fermion Ψ using these fields as coefficients in an expansion over the Clifford algebra of Dirac gamma matrices

$$\Psi = \phi I + \phi_\mu \gamma^\mu + \phi_{\mu\nu}\gamma^\mu\gamma^\nu + \ldots + \phi_{\mu_1\mu_2\ldots\mu_D}\gamma^{\mu_1}\gamma^{\mu_2}\cdots\gamma^{\mu_D} \tag{3}$$

It is then straightforward to show that Ψ satisfies the usual Dirac equation $(\gamma^\mu\partial_\mu + m)\Psi = 0$ and hence the fermionic content of the flat space theory is equivalent to a set of $2^{D/2}$ degenerate Dirac fermions corresponding to the columns of Ψ. However, in a curved space this equivalence to the Dirac equation is lost.

A key advantage of KD fermions over Dirac fermions is they may be coupled to gravity without introducing frames and spin connections and may be discretized without inducing fermion doubling. Indeed one merely maps the p-form fields to lattice fields defined on p-simplices in a triangulation (p-cochains) and replaces d and $d^\dagger$ by boundary δ and coboundary $\bar{\delta}$ operators respectively, which have a natural action on such p-cochains—see [1,2] and [3–5] for details.

In our work, we have focused on studying the back reaction induced on the gravitational theory as a

[*]masaduzzaman@uiowa.edu
[†]smcatterall@gmail.com
[‡]asamlodia@gmail.com

Published by the American Physical Society under the terms of the Creative Commons Attribution 4.0 International license. Further distribution of this work must maintain attribution to the author(s) and the published article's title, journal citation, and DOI. Funded by SCOAP[3].

consequence of the presence of KD fermions and particularly its effect on the holographic properties of the system. We employ both analytic arguments and Monte Carlo simulation to infer the phase diagram of the theory. We find, for a large number of fields N, the effect of the fermions is to suppress curvature fluctuations. In the limit that $N \to \infty$, we find that the geometry becomes a classical constant (negative) curvature space corresponding to a regular tessellation of two-dimensional hyperbolic space.

Furthermore, we show in this limit, that boundary-boundary correlation functions exhibit a power law decay as expected for a holographic theory. Indeed, the dependence on bulk mass matches well with continuum predictions [6]. However, we will argue that this behavior does not survive if the number of fields is held fixed in the thermodynamic limit—the discrete geometries become disordered as the area of the disk increases and the simple holographic behavior of the correlators is lost.

II. MODEL

The partition function for the model is written as,

$$\begin{aligned} Z &= \sum_{\mathcal{T}\in \text{disk}} \int D\bar{\Phi} D\Phi e^{\bar{\Phi} K(\mathcal{T}) \Phi} e^{-S_g} \\ &= \sum_{\mathcal{T}\in \text{disk}} \prod_{p=0}^{D} \det{}^{N/2} \left(\Box^{(p)}(\mathcal{T}) + m^2\right) e^{-S_g} \\ &= \sum_{\mathcal{T}\in \text{disk}} e^{-S_{\text{eff}}} e^{-S_g} \end{aligned}$$

$$\text{where } S_{\text{eff}} = -\frac{N}{2} \sum_{p=0}^{D} \text{Tr} \ln \left(\Box^{(p)}(\mathcal{T}) + m^2\right) \tag{4}$$

where we have included N flavors of KD fermion and the two-dimensional bare gravitational action is just given by a cosmological constant term $S_g = \kappa N_2$ where N_2 is the number of triangles. In practice, we consider triangulations of the disk $\mathcal{T}$ with a fixed number of triangles so this term plays no role. The square of the KD operator yields an operator which is the direct sum of Laplacians $\Box^{(p)}$ for each type p of simplices (vertices, links, and triangles) and hence appear in the effective action arising from the fermion loops. The sum over $\mathcal{T}$ includes all combinatorial triangulations with a boundary structure that corresponds to the last layer of a finite $\{3, 7\}$ tessellation of hyperbolic space [7]. That is, we impose the discrete equivalent of asymptotic AdS boundary conditions on the geometry. As a consequence, the average bulk curvature is fixed to a negative constant while a Dirichlet boundary condition is used for the fermions.

III. ANALYTIC ANALYSIS

It is instructive to analyze the model first in the large mass limit $m \to \infty$. Furthermore, let us restrict our attention to the contributions of the $p = 0$ (node) sector of the fermion operator whose matrix elements take the form

$$M_{ij} = \Box^{(0)}_{ij} + \delta_{ij} q_i m^2 = (1 + m^2) q_i \delta_{ij} - C_{ij} \tag{5}$$

where q_i denotes the number of neighbors of the ith node and $C_{ij} = 1$ if nodes i and j are neighbors. It is easy to factorize this in the form $M = QAQ$ where the matrix Q is diagonal with matrix elements $\sqrt{q_i}$ and A takes the form

$$A_{ij} = (1 + m^2)\delta_{ij} - \frac{C_{ij}}{\sqrt{q_i q_j}}. \tag{6}$$

Thus

$$\det(M) = e^{N_0 \ln(1+m^2)} \left(\prod_i^{N_0} q_i \right) e^{\sum_L \frac{1}{L} \frac{1}{(1+m^2)^L} \Omega_L} \tag{7}$$

where Ω_L is the number of closed loops of length L that can be drawn on the triangulation with each loop weighted by the inverse of the product of the q_i for each vertex in the loop. Taking the large m limit we find that the effective action for KD fermions contains the local term

$$S_{\text{eff}} = -\frac{N}{2} \sum_{i \in \text{bulk}} \ln(q_i) \tag{8}$$

Using the usual expression for the scalar (Regge) curvature associated with each node in a triangulation $R_i = \frac{\pi}{q_i}(q_i - 6)$ this can be rewritten

$$-\frac{N}{2} \ln(q_i) = \text{const} + N \sum_{i \in \text{bulk}} \frac{1}{\pi^2} R_i^2 + \cdots \tag{9}$$

Thus the leading effect of the fermion backreaction in the large mass limit is to induce a R^2 operator that suppresses local curvature fluctuations. For large N this conclusion can be reinforced by performing a steepest descent evaluation of this leading contribution by solving

$$\frac{\partial S_{\text{eff}}}{\partial q_i} = 0 \quad \text{with} \quad \sum_i q_i = \text{fixed}. \tag{10}$$

This generates a homogeneous solution with $q_i = 7$—this value being determined by the geometrical boundary conditions—here the fact that the boundary nodes have a connectivity determined by the final layer of a $\{3, 7\}$ tessellation.

At $m = 0$ one can find another representation of the determinant of the node Laplacian in terms of the number of spanning trees in the corresponding graph. Thus as $N \to \infty$ we expect the partition function to be dominated by the triangulation with the maximal number of

spanning trees—the regular tessellation with constant local curvature [8]. Thus for large N and for both small and large fermion mass we expect the partition function to be dominated by regular tessellations of two dimensional hyperbolic space. We will see that this expectation is indeed borne out in our simulations.

Let us now examine the expected behavior of fermion boundary-boundary correlation functions on such regular tessellations. We will concentrate on the node correlators although our conclusions will apply equally to all components of the fermion correlator. This correlation function can be written

$$\langle \phi_i \phi_j \rangle = \left(\frac{-K + m}{-\Box + m^2} \right)_{ij} \tag{11}$$

where $K = \delta - \bar{\delta}$. Focusing on the piece proportional to m we see that it can be written as a matrix element of the inverse lattice Laplacian. Thus

$$\langle \phi_i \phi_j \rangle \sim \frac{1}{m} \left(1 - \frac{1}{m^2} \Box \right)^{-1}_{ij} \tag{12}$$

For large mass we can expand the inverse operator in powers of $1/m^2$. Each successive term connects nodes one further step apart in the lattice. The first nonzero contribution to this correlator then arises from the power of $\Box$ that corresponds to the shortest path on the lattice between the two boundary nodes—the lattice geodesic. For a regular hyperbolic lattice this path runs through the bulk and is of length $\ln r$ where r is the boundary separation. The correlator is then

$$\langle \phi_i \phi_j \rangle \sim \left(\frac{1}{m^2} \right)^{\ln r} \sim \frac{1}{r^{2\Delta}} \quad \text{with} \quad \Delta = \ln m^2. \tag{13}$$

Thus holographic behavior is expected for any value of the bulk mass at least as $m \to \infty$. It is not hard to generalize this argument to show that the strong coupling limit of *any* lattice spin or gauge model formulated on a tessellation of hyperbolic space will exhibit holographic behavior—see [9]. Using Monte Carlo simulation we will see that in fact this behavior extends to all values of m provided the geometry is homogeneous as was seen earlier in [10,11].

According to the AdS/CFT correspondence, the relationship between the mass m of a scalar field in the bulk of AdS_{d+1} and the scaling dimension Δ of the boundary field operator is given by the following equation [6],

$$\Delta(\Delta - d) = (mL)^2 \tag{14}$$

where d is the dimension of the boundary and L the AdS curvature. Two solutions exist for this equation which are,

$$\Delta_\pm = \frac{d}{2} \pm \sqrt{\frac{d^2}{4} + (mL)^2}. \tag{15}$$

Using appropriate boundary conditions, one can get back either one of the solutions [6]. Dirichlet boundary conditions as used here ensure the Δ_+ solution is obtained.

This continuum prediction holds only for a classical homogeneous hyperbolic/AdS space. One of the goals of our study is to see whether this behavior survives in the presence of bulk quantum gravity fluctuations. In our model the magnitude of the latter can be adjusted by dialing the number of fermions propagating on the geometry. We have argued that in the limit $N \to \infty$, the background geometry will reduce to a hyperbolic geometry with constant local curvature and this is borne out by our simulations which are discussed in the next section.

IV. MONTE CARLO SIMULATIONS

In order to do Monte Carlo simulations capable of reproducing a path integral over bulk geometries we need a set of local moves that change the triangulation $\mathcal{T}$. A suitable set of moves are called the Pachner moves and can be implemented in any dimension—see Ref. [12] for a simple implementation of such moves in D dimensions. In two dimensions one such move—the so-called link flip move (see Fig. 1)—is known to be ergodic in the space of random triangulations of fixed area. By choosing to perform this move at random one can construct a Metropolis procedure that is capable of performing a random walk in the space all such triangulations $\mathcal{T}$ weighted by the effective action. Figure 2 shows typical random geometries generated in Monte Carlo sampling, where near regular tessellations are obtained when N is large. The change in the effective action needed by the Metropolis algorithm requires the evaluation of the change in the fermion determinants under such link flip moves. We have used the SuperLU package to compute the change in these determinants [13]. This is efficient but still scales like the cube of the system volume which limits us to relatively small lattices. In practice we have simulated a range of lattice areas up to 1162 lattice sites using variables numbers of KD fermions and using a set of masses that extend from near massless $m = 0.0001$ to $m = 10.0$. Typical Monte Carlo ensembles for a fixed set of parameters

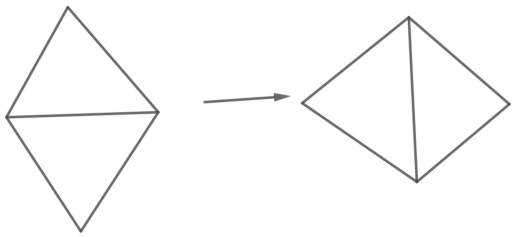

FIG. 1. Link flip Move.

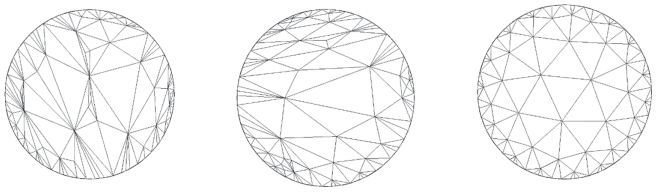

FIG. 2. Typical geometries arising in Monte Carlo simulations. The disk on the right is a near perfect regular tessellation for large N case.

correspond to 1000 configurations obtained from 20 000 Monte Carlo sweeps with a gap of 20.

V. SIMULATIONS AND RESULTS

A. Bulk observables

In this subsection, we first investigate the bulk geometrical properties of the triangulations. Figure 3, which plots the fluctuations in the local curvature $Q = \langle (q-7)^2 \rangle$ averaged over the bulk nodes as a function of the number of fields N, shows clearly that in the $N \to \infty$ limit, the geometry indeed approaches the regular $\{3, 7\}$ tessellation of hyperbolic space corresponding to a continuum space with constant negative curvature. However, it can be seen that the number of fields that are needed to freeze the lattice geometry to the regular tessellation depends on both the mass m and the lattice area N_2. Figure 4 shows a plot of the bulk value of Q vs the bulk mass for $N = 2$–512. Clearly one needs larger N as m increases to smooth the lattice geometry at fixed area. This makes sense; if one integrates out massive fields one would expect to generate local R^2 operators as we saw for $m \to \infty$. However for finite mass there will be $1/m^2$ corrections arising from the expansion over closed loops which reduce the effective R^2 coupling. However this coupling will also be proportional to the number of KD fields so the latter can be increased to compensate for this—an effect which is visible in the plot.

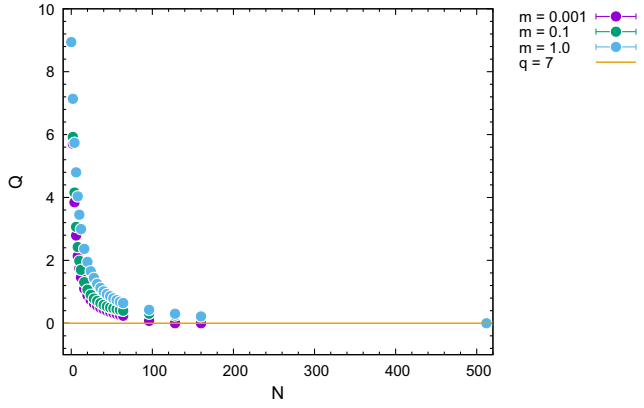

FIG. 3. Curvature fluctuation Q vs number N of KD fermions with different bulk masses m for a lattice consisting of $N_2 = 1162$ triangles.

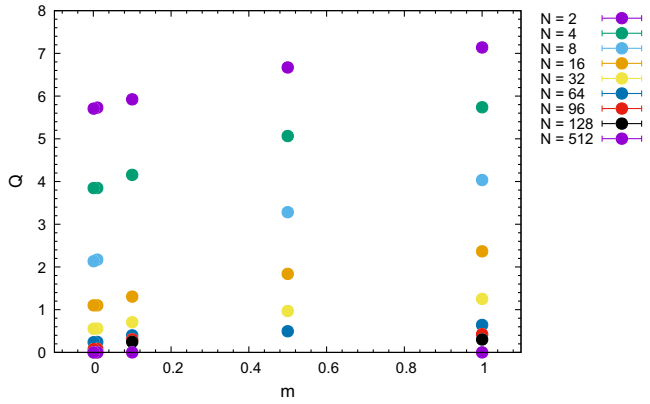

FIG. 4. Q vs m_{bulk} with different number of fields N for a lattice with $N_2 = 1162$ triangles.

Indeed, since R^2 is an irrelevant operator in two dimensions one might expect its coupling to flow to zero in the infrared and hence to vanish in the thermodynamic limit rendering the bulk lattice geometries disordered for any finite number of *massive* fermions. In light of this it is interesting to ask what happens for vanishing mass as the area is increased. Figure 5 shows a plot of Q vs the lattice area for several values of the bulk mass m including the small mass limit. It is clear that the value of Q indeed starts to grow as the area increases for any value of the mass which is consistent with our earlier argument.

One can also understand this effect via the following argument. Imagine the effect of a single link flip around the regular tessellation. It is not hard to verify that this changes the action $\Delta S_{1\text{flip}} = \alpha$ where $\alpha = \mathcal{O}(1)$ and is *independent* of the area N_2. However there are many ways to make such a fluctuation—the link flip can occur on any bulk link. Thus the entropy associated to such a flipped configuration increases logarithmically with the area. Putting these two facts together one sees that the change in the free energy associated with a single link flip $\Delta F = \alpha - \beta \ln N_2$ can be made arbitrarily negative by link flips for large enough area. Thus one expects, even in the massless case,[1] that link flips will predominate for fixed N in the large area limi—as we see in the data. Indeed, this implies that the regular tessellation will *not* dominate in the limit of large areas *unless* one sends $N \to \infty$.

Thus our analysis of bulk local observables suggests that typical geometries become disordered in the thermodynamic limit. We explore the consequences of this for holography in the next section.

[1]In practice $m = 0.001$ gives a good approximation to the massless theory on our lattices. We have checked that neither bulk or boundary observables change on further decrease of m.

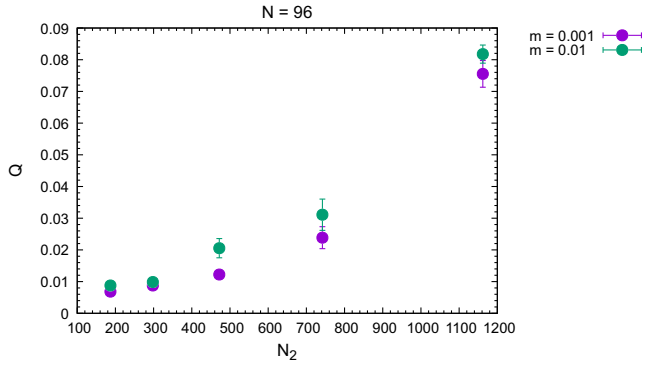

FIG. 5. Q vs area N_2 for fixed $N = 96$ and different bulk masses.

B. Boundary correlators

The boundary correlation functions are computed as matrix elements of the inverse KD operator including the bulk mass term[2]

$$C(r) = \sum_{ij} \frac{1}{n_{ij}(r)} \delta_{|i-j|,r} (-\Box + m^2)^{-1}_{ij} \tag{16}$$

where $|i - j|$ is the boundary distance (in units of the lattice spacing) between boundary sites i and j and

$$n_{ij}(r) = \sum_{ij} \delta_{|i-j|,r} \tag{17}$$

In practice we assess errors on our correlation functions by a jackknife procedure. Typically we have used $N_{\text{jack}} = 200$ samples to assess statistical errors. The boundary correlators for smaller N suffer from large fluctuations as the boundary geodesic distance increases. These fluctuations become more significant for larger bulk mass.

To handle this and remove the leading discretization effects we have also performed a smoothing operation on the correlation function before attempting power law fits. This entails averaging the correlators at any distance over a block of a certain size centered on that distance. We have checked that our results are robust to the size of this parameter. Once this is done we fit the resultant correlator to a power law to extract Δ.

An example of this procedure can be seen in Fig. 6 which shows the smoothed correlation function and fit for $N = 512$ and $m = 1.0$. In this plot we have chosen to fit the data in a particular window of length 20 lattice spacings. We plot the data versus $\ln(1 - \cos\theta)$ where $\theta = \pi \frac{r}{r_{\text{max}}}$ and r_{max} is the maximum boundary geodesic distance (half of the total length of the boundary). This takes into account the leading

[2]To compute the correlators we use open boundary conditions but include a very large boundary mass for the fermions to drive the magnitude of the boundary field close to zero. Typically $m^2_{\partial D} = 1000.0$.

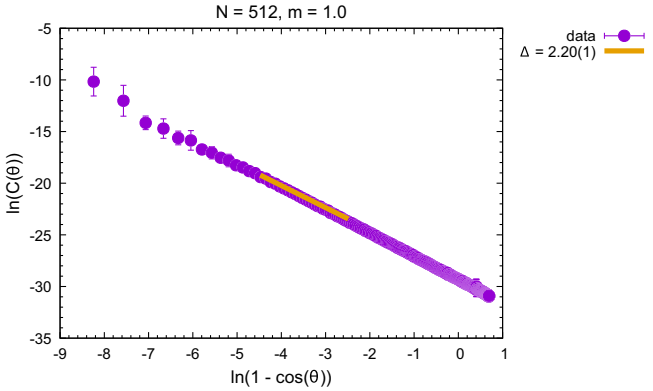

FIG. 6. Correlation function for $N = 512$ and $m = 1.0$ using smoothing block size $b = 4$ and a fitting window of size 20.

finite size effects. For $r_{\text{max}} \to \infty$ this is just $2 \ln r$. For large N the results are somewhat insensitive to the choice of window. But this is no longer true as N is reduced. For example Fig. 7 shows a correlator for $m = 1.0$ at $N = 2$ for several different values of the total area. In this case the log-log plot shows a pronounced curvature and a strong finite size effect and it is far less clear which fitting window should be chosen.

To establish robust values for any extracted Δ we need to determine what fitting window to use. To do this we have determined an effective running Δ at each distance r and look for a robust fitting window where consistent values of Δ are obtained independent of the precise location of the window. In more detail, we fix the fitting window size and move the fitting window progressively out to larger distances keeping both the block size b and number of points N_{fit} fixed. For each choice of fitting window, we fit a power law from $\ln C(r)$ vs $\ln r$ and extract an estimate of the local power law exponent Δ. We then look for a plateau in the value of Δ indicating a simple power law decay. We additionally check that the resultant fits have an acceptable χ^2 per degree of freedom (see the appendix for a plot of χ^2 vs the fitting window) To test this method we first restrict ourselves to the case

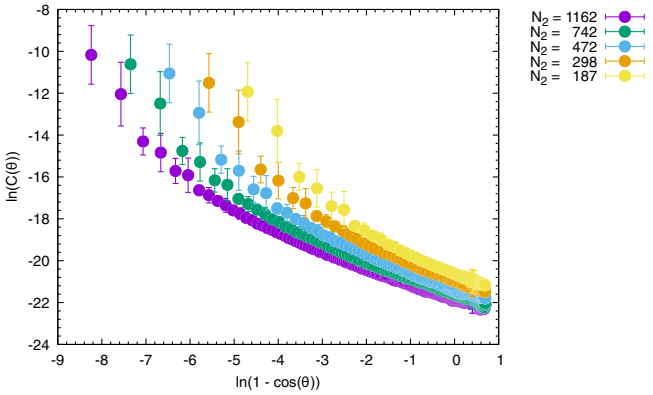

FIG. 7. Correlation function for $N = 2$ and $m = 1.0$ with smoothing block size $b = 4$ for different number of simplices.

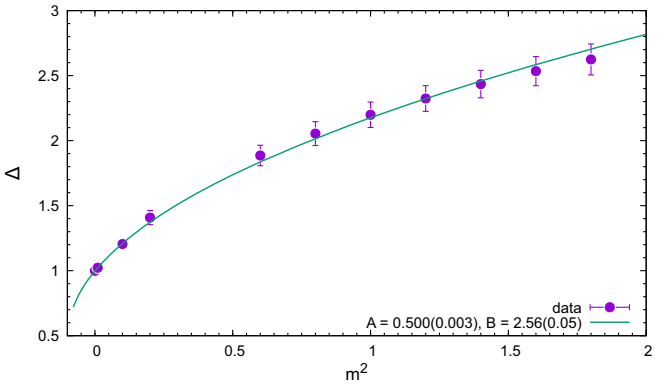

FIG. 8. Δ vs m^2 at $N = 512$ and $N_2 = 1162$. The χ^2 per degree of freedom for this fit is 0.16.

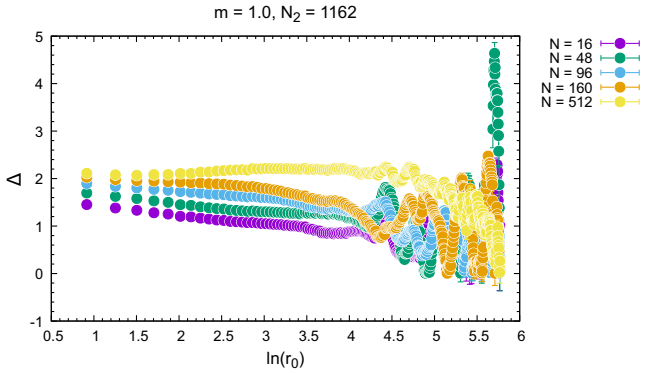

FIG. 9. Δ vs location of fitting window for $N_2 = 1162$ and $m = 1.0$ ($N_{\text{fit}} = 20$).

of $N = 512$ where the lattices are perfect regular $\{3, 7\}$ tessellations of the hyperbolic plane for all masses and lattice sizes we employed. Figure 8 plots Δ versus m^2 for $N = 512$. The fit we show corresponds to the continuum prediction given in Eq. (15). We fit the data with the form: $\Delta = A + \sqrt{A^2 + Bm^2}$. From the fit we find $A = 0.500 \pm 0.003$ and $B = 2.558 \pm 0.051$. B is related to the radius of curvature $L = \sqrt{B/2} = 1.131 \pm 0.022$. This can be compared with that expected for a $\{p, q\}$ tessellation of hyperbolic space given by

$$\frac{1}{L} = 2\cosh^{-1}\left(\frac{\cos(\pi/p)}{\sin(\pi/q)}\right) \tag{18}$$

where $p = 3$ and $q = 7$ for a triangulation. The formula yields $L = 0.917$ which differs by $\mathcal{O}(10)\%$ from the theoretical prediction which we attribute to finite size effects.[3]

Let us now turn to the situation at finite N. Figure 9 shows the value of Δ extracted from simulations at

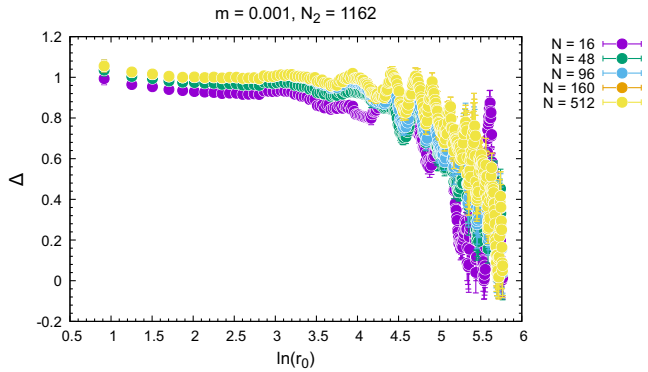

FIG. 10. Δ vs location of fitting window for $N_2 = 1162$ and $m = 0.001$ ($N_{\text{fit}} = 20$).

$m = 1.0$, area $N_2 = 1162$ for several values of N. We fix the fitting window to 20 with r_0 the starting point of the fit and the block size to $b = 4$. It should be clear that only for $N = 512$ do we see a reliable plateau while for smaller N the effective scaling dimension Δ runs with distance. We interpret this as a breakdown in holography. In appendix C we show that this conclusion does not depend on the size of the fitting window N_{fit}.

Figure 10 shows a similar plot for $m = 0.001$. In this case a plateau is visible even for small values of N[4] Thus we conclude that the boundary theory remains conformal for massless fermions even in the presence of bulk disorder although the scaling dimension of the field appears to receive quantum gravity corrections. We discuss the possible reasons for this in our conclusions. Figures 12, 13, and 14 in Appendix C shows the roubustness of the results for Δ on the size of the fitting window by choosing $N_{\text{fit}} = 12$.

VI. SUMMARY AND CONCLUSION

We have shown that the back reaction of KD fermions on a two-dimensional quantum geometry with the topology of a disk is such as to suppress local curvature fluctuations. Indeed, for $N \to \infty$ limit, we find the lattice geometries approach that of a regular tessellation of hyperbolic space—in the limit a classical space with constant negative curvature. Furthermore, in this limit, the boundary correlation functions exhibit a holographic property falling off as powers of the boundary distance. Remarkably the dependence of this power on bulk fermion mass matches quite closely the continuum prediction.

However, if the number of fields is held fixed, we have provided evidence that fluctuations of the geometry reemerge in the thermodynamic limit both for massive and massless fields. For massive fermions the boundary

[3]The factor of $\sqrt{2}$ connecting B to L arises from a dual lattice parameter that is needed to construct the correct kinetic operator for the scalar field on a tessellation [7,14,15].

[4]Figure 11, in Appendix B we show a typical correlator in the small mass limit which reinforces the notion that one can obtain a good power law fit over a wide range of fitting windows.

correlators, while the correlation is relatively long-ranged, no longer fit a simple power law. We tentatively conclude that in this regime the model no longer exhibits a holographic phase. This is not too surprising—as we have shown, integrating out massive fields produces local operators such as R^2 which are irrelevant at long distances. The path integral is then dominated by metrics that differ drastically from classical hyperbolic space.

The case of massless fermions is more subtle—in this case, nonlocal operators can arise in the gravity action. For example the Polyakov action can be generated [16,17]

$$S_{\mathrm{P}} = \int d^2x\sqrt{g(x)} \int d^2y\sqrt{g(y)}R(x)\Box^{-1}(x-y)R(y) \tag{19}$$

where $\Box$ is the covariant Laplacian and R the Ricci scalar. In the continuum we can fix the conformal gauge $g = e^{2b\phi}\hat{g}$ and obtain the well known Liouville action [16]:

$$S = \frac{1}{4\pi}\int d^2x\sqrt{\hat{g}}[(\partial\phi)^2 + Q\hat{R}\phi] \tag{20}$$

where $Q = b + b^{-1}$ is related to the Liouville central charge $c_L = 1 + 6Q^2$. The entire system is quantum conformal invariant if $c_M + c_L = 26$ where 26 arises from the ghosts needed to gauge fix diffeomorphism symmetry. Notice that while KD fermions are equivalent to multiples of Dirac fermions in flat space this is no longer true in the presence of gravity where they behave like ghosts. Indeed, for KD fermions, the central charge $c_M \to -\infty$ as $N \to \infty$ and we are within the regime of applicability of Liouville theory with Q large and b small corresponding to weak gravity. In this limit, we expect that conformal invariance is maintained with boundary correlation functions still falling off as a power of the distance [17] even though the bulk geometry no longer corresponds to a classical hyperbolic space. This conclusion agrees with our simulations.

ACKNOWLEDGMENTS

Numerical computations were performed at Syracuse University HTC Campus Grid under NSF Grant No. ACI-1341006. We acknowledge support from U.S. Department of Energy Grants No. DE-SC0019139 and No. DE-SC0009998.

TABLE I. Data for Δ vs m^2 at $N = 512, N_2 = 1162$. σ is the error in estimation Δ.

m^2	Δ	σ	χ^2/d.o.f
0.000001	0.99936	0.00265	0.2469
0.0001	0.99959	0.00264	0.24682
0.01	1.02274	0.002	0.24036
0.1	1.20491	0.00805	0.21221
0.2	1.4084	0.00834	0.35023
0.6	1.88571	0.00975	0.30089
0.8	2.05425	0.01059	0.28498
1.0	2.19882	0.01066	0.29197
1.2	2.32405	0.01059	0.30889
1.4	2.43486	0.011	0.32482
1.6	2.53427	0.0117	0.34371
1.8	2.62441	0.01274	0.36496

APPENDIX A: FITS FOR Δ

Below we show the result of fitting Δ for various fermion masses for a large number of fermions and an area $N_2 = 1162$.

APPENDIX B: MASSLESS FERMION CORRELATORS

Here we show a boundary correlator for small $N = 2$ and in the (near) massless regime $m = 0.001$. A clear linear regime for large values of $\ln(1 - \cos(\theta))$ or r indicates a good robust power law fit.

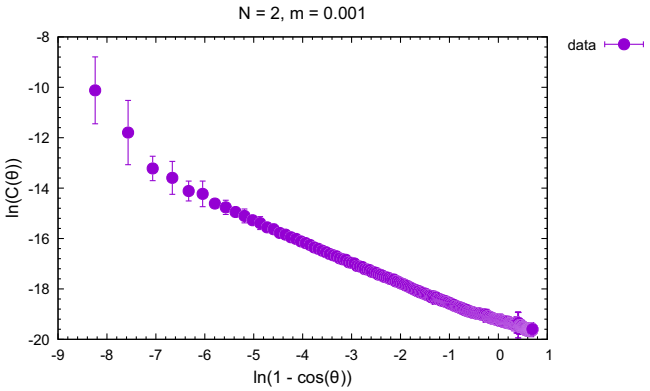

FIG. 11. Boundary correlator with smoothing block size $b = 4$f for $N = 2$, $N_2 = 1162$ and $m = 0.001$.

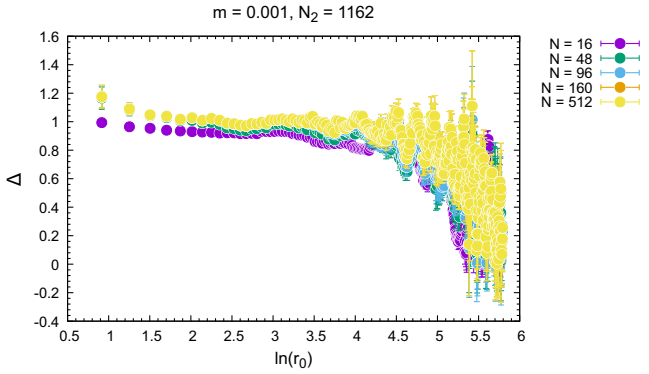

FIG. 12. Scaling dimension Δ for fitting window $N_{\text{fit}} = 12$ with $N_2 = 1162$ and $m = 0.001$ for a variety of N.

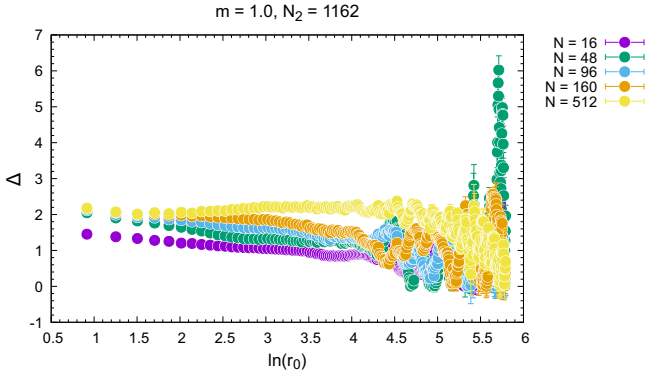

FIG. 13. Scaling dimension Δ for fitting window $N_{\text{fit}} = 12$ with $N_2 = 1162$ and $m = 1.0$ for a variety of N.

APPENDIX C: VARYING THE FITTING WINDOW

In the pictures below we show the robustness of our results for Δ on the size of the fitting window by choosing $N_{\text{fit}} = 12$ in contrast to the choice $N_{\text{fit}} = 20$ used in the main text.

In the following plot we show the χ^2 of a typical correlator fit as a function of the fitting window.

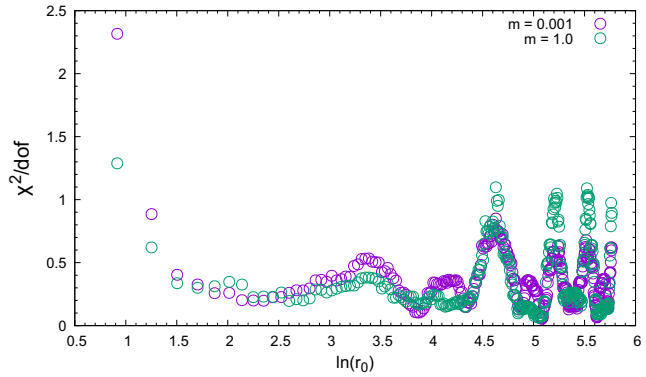

FIG. 14. χ^2 vs the fitting window for $N = 512$ and $m = 1.0$.

[1] T. Banks, Y. Dothan, and D. Horn, Phys. Lett. **117B**, 413 (1982).
[2] J. M. Rabin, Nucl. Phys. **B201**, 315 (1982).
[3] S. Catterall, arXiv:2311.02487.
[4] S. Catterall, Phys. Rev. D **107**, 014501 (2023).
[5] N. Butt, S. Catterall, A. Pradhan, and G. C. Toga, Phys. Rev. D **104**, 094504 (2021).
[6] I. R. Klebanov and E. Witten, Nucl. Phys. **B556**, 89 (1999).
[7] M. Asaduzzaman, S. Catterall, J. Hubisz, R. Nelson, and J. Unmuth-Yockey, Phys. Rev. D **102**, 034511 (2020).
[8] D. V. Boulatov, V. A. Kazakov, I. K. Kostov, and A. A. Migdal, Nucl. Phys. **B275**, 641 (1986).
[9] M. Asaduzzaman, S. Catterall, J. Hubisz, R. Nelson, and J. Unmuth-Yockey, Phys. Rev. D **106**, 054506 (2022).
[10] M. Asaduzzaman and S. Catterall, Proc. Sci. LATTICE2021 (**2022**) 430, https://doi.org/10.48550/arXiv.2112.00927.
[11] M. Asaduzzaman, S. Catterall, J. Hubisz, R. Nelson, and J. Unmuth-Yockey, Proc. Sci. LATTICE2021 (**2022**) 016.
[12] S. Catterall, Comput. Phys. Commun. **87**, 409 (1995).
[13] J. W. Demmel, S. C. Eisenstat, J. R. Gilbert, X. S. Li, and J. W. H. Liu, SIAM J. Matrix Anal. Appl. **20**, 720 (1999).
[14] R. C. Brower, C. V. Cogburn, A. L. Fitzpatrick, D. Howarth, and C.-I. Tan, Phys. Rev. D **103**, 094507 (2021).
[15] R. C. Brower, C. V. Cogburn, and E. Owen, Phys. Rev. D **105**, 114503 (2022).
[16] J. Distler and H. Kawai, Nucl. Phys. **B321**, 509 (1989).
[17] T. G. Mertens and G. J. Turiaci, J. High Energy Phys. 01 (2021) 073.